

# The Design of Long-Term and Short-Term Guided Wave Structural Health Monitoring Systems

G. KONSTANTINIDIS, B. W. DRINKWATER, P. D. WILCOX

Department of Mechanical Engineering, University of Bristol, Bristol, United Kingdom

**Abstract.** Guided acoustic waves offer the potential for structural health monitoring (SHM) with an extremely low sensor density. They are attractive as they can travel large distances in structures and have been shown to be sensitive to defects such as cracking, corrosion in metals and delamination in composites. However, in all but the most simple structures the wave interactions with structural features become too complex for the time domain signals to be interpreted directly. One approach to overcoming this complexity is to subtract a baseline reference signal from the measured system and monitor changes in the response. Inevitably the performance of such a SHM system is then governed by the stability of the measured signal relative to this reference. In the short-term the stability of such a system is shown to be good, leading to the possibility of characterizing rapidly growing defects such as impact damage in composites and some types of cracking. In the long-term the performance is shown to degrade with various environmental variables such as the ambient temperature. This has serious implications for the viability of this approach in an industrial setting. Methods for improving the long-term performance are then discussed and their potential demonstrated.

## Introduction

Permanently installed structural health monitoring (SHM) systems provide information on the physical condition of a structure. This information can be used for various purposes such as estimating remaining life, modifying the allowable operating envelope of the structure, timing the next maintenance shutdown, and allowing scheduled non-destructive evaluation (NDE) and repair work to be targeted. SHM can be subdivided into usage monitoring and damage detection. Usage monitoring includes, for example, strain gauge systems that record the loading history to which the structure is subjected from which remaining life predictions can be made. However, usage monitoring does not provide information about unexpected damage initiation and growth and hence some form of damage detection is still required. In some cases, likely locations of possible damage such as corrosion or fretting fatigue may be known and the necessary damage detection sensors can be installed at appropriate locations. However, there are many structures where unexpected critical damage may occur anywhere in the structure. Examples include impact damage causing hidden delaminations in a composite aircraft structure and localized corrosion pitting in power generation and petrochemical plant. These situations provide the motivation for the development of SHM systems that can detect localized damage throughout a structure. The benefits of SHM in aerospace applications have been discussed by Boller [1].

The guided wave regime represents an attractive compromise between sensitivity to damage and detection range. Guided waves have documented sensitivity to a range of types of damage including cracks [2, 3], corrosion [4] and delaminations [5]. Deployable guided wave systems are already used in NDE applications for the inspection of geometrically simple waveguide structures such as pipes [6], plate [7] and rails [8]. In more complex structures, such as airframes, the difficulty in interpretation of signals due to the multitude of reflections from structural features has prevented the development of deployable systems. However, in a structural health monitoring (SHM) context where permanently attached sensors are used, the issue of signal interpretation is potentially surmountable by using baseline signal subtraction. Fundamental to this approach is the sensitivity and stability of the subtraction approach.

The current paper begins by describing the overall strategy proposed for damage detection with guided waves using a simple structure as an example. An experimental example is used to give a quantitative indication of the level of sensitivity desirable and the sensitivity achievable with the basic baseline subtraction approach. This provides the motivation for quantifying how benign changes to the environment, such as temperature, affect the sensitivity of the baseline subtraction approach and investigating possible strategies for its improvement.

## **Overall Strategy**

The strategy proposed for guided wave structural health monitoring is to instrument the structure with a sparse array of simple guided wave sensors. One sensor initially acts as a transmitter and injects a burst of guided wave energy into the structure and the other sensors act as receivers. Transmission then switches to the next sensor and continues until the time-domain signals from every possible sensor pair have been recorded. This set of time-domain signals is referred to as a data-set. Each signal in the data-set contains both a directly transmitted signal between transmitter and receiver followed by a number of reflected signals.

From a single data-set it is almost impossible to obtain useful information about even the most simple structure due to the number of reflected signals. The strategy is therefore to look for differences between data-sets and this is the so-called baseline subtraction approach. If damage occurs to the structure between the acquisition of the data-sets then, in principle, the only signals that remain after subtracting the baseline (first) data-set from the second data-set are artefacts of the damage. Possible detection, quantification and localization strategies, for the damage, can then be devised and applied to the data-set after subtraction of the baseline data-set. In this paper, the application of this approach to a simple aluminium plate using the  $A_0$  Lamb wave mode is discussed. It should be stressed that the choice of structure and mode has been made for convenience; the underlying principles are general.

## **Experimental Demonstration of Damage Detection**

### *2.1 Experimental apparatus*

The structure used in the experimental example is a 1 m by 1.5 m by 3 mm thick aluminium plate. The sensors are three 5 mm diameter by 2 mm thick piezoelectric disks bonded to the plate in a triangle layout as shown in Fig. 1. The transducers are poled in the thickness direction and the excitation is by a 5 cycle Hanning windowed tone-burst with a centre

frequency of 250 kHz. With this excitation signal and at this frequency the transducers are most sensitive to the  $A_0$  Lamb wave mode although the  $S_0$  Lamb wave mode is also excited and detected to a lesser degree. In order to reduce the random noise components, a bandpass filter is applied to the received time traces to eliminate any low or high frequency noise.

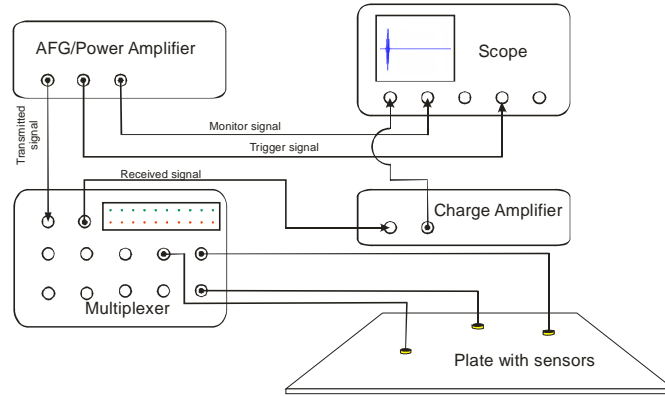


**Figure 1:** Experimental equipment used for imaging experiments

## 2.2 Results

The baseline data-set was acquired on the damage-free plate and the baseline image, shown in Fig 2(a) was produced (see [9, 10] for a fuller description of the imaging algorithm). It is not possible to interpret this image directly. Immediately after this data-set was recorded, a second data-set was acquired, without modification of the plate, and a second image, generated. The amplitude of the total difference image, between these two seemingly identical images is shown in Fig. 2(b) to provide an indication of signal to noise ratio (SNR) achievable. Both images in Fig. 2 are plotted on the same dB scales, where 0 dB corresponds to the size of the largest signal in Fig. 2(a), which is the reflection from the plate edge. It can be seen that a SNR of over 55 dB has been obtained over the majority of the image area in Fig. 2(b) with isolated peaks around 40 dB.

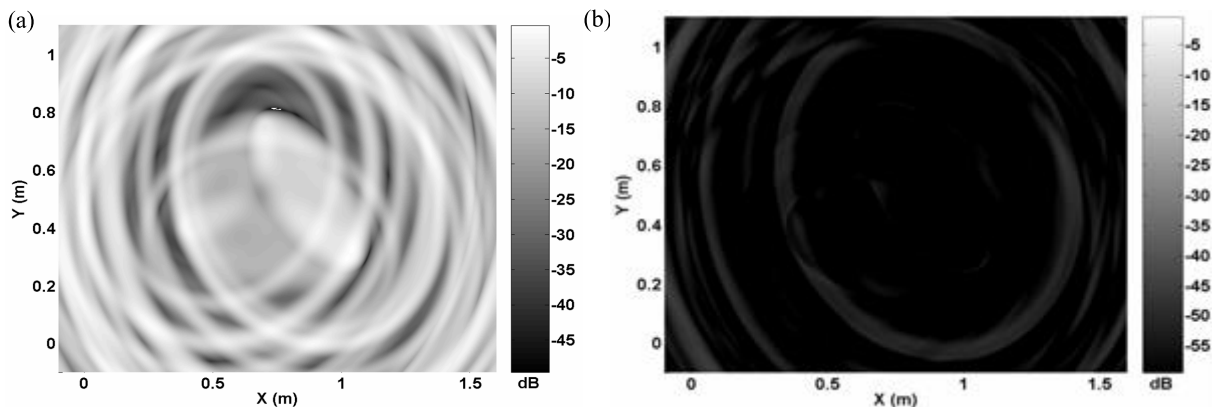


**Figure 2:** (a) Baseline image, from aluminium plate; (b) total difference image, between second image, obtained without modification of the plate and baseline image. The dB scale is with respect to the same origin (0 dB) in both images.

The plate was then “damaged” by the addition of a 22 mm diameter steel ball bonded to the plate surface to cause guided wave reflections of comparable amplitude to those that might be caused by localized damage. The positive and negative difference

images, obtained after baseline subtraction for a data-set recorded after the introduction of the damage are shown in Figs. 3(a) and (b). As anticipated, a definite peak is visible in Fig 3(a) at the location of the damage as indicated by the white circle. The amplitude of this peak is -35 dB below that of the reflected signal from a plate edge.

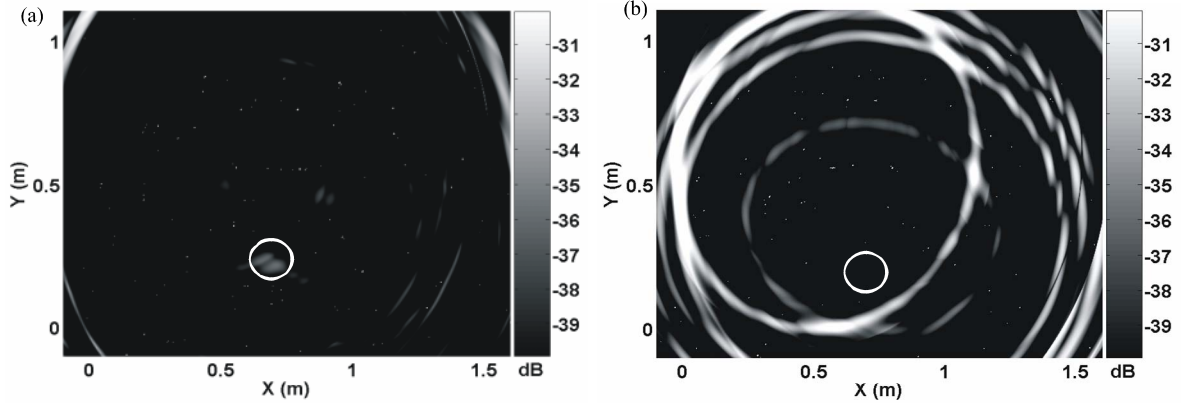


**Figure 3 :** (a) Positive difference image, and (b) negative difference image, after baseline subtraction on a damaged plate. The dB scale is with respect to the same origin (0 dB) in both images and is the same as that in Fig.2

In order for damage to be reliably detected the underlying SNR must typically be 6 dB smaller than the signal from the damage, therefore the SNR of the baseline subtraction must be greater than approximately 40 dB (with respect to an edge reflection) to be useful. The results were obtained under laboratory conditions on a well controlled sample with only a few minutes between the acquisition of the baseline data-set and the subsequent data-set. It has been observed that when the time between the acquisition of data-sets increases, the performance of the baseline subtraction deteriorates. In the next section this deterioration is quantified and its causes identified.

## Quantification of Baseline Subtraction Approach

### 3.1 Experimental measurements

The sensitivity of the baseline subtraction approach is dependent on the stability of the individual time-domain signals in a data-set. For convenience only the time-domain signal between one pair of transducers is studied; the effect of combining multiple signals to form an image simply yields a few extra dB of signal to noise ratio due to averaging effects.

To quantify the difference between two nominally identical time-domain signals, the error,  $E(t)$ , is introduced:

$$E(t) = 20 \log_{10} |h^{(1)}(t) - h^{(0)}(t)| \quad (1)$$

where  $h(t)$  is the filtered and distance-compensated Hilbert envelope of the corresponding time-domain signal, normalized to the first  $A_0$  arrival following the procedure. The maximum value of the  $E(t)$  is computed over various zones in the time-domain signal as shown in Fig. 4 that correspond to (a) incoherent noise before the transmitted signal, (b) the direct arrival of the  $S_0$  mode, (c) the direct arrival of the  $A_0$  mode and (d) the remainder of the time-domain signal that contains multiple edge reflections.

It was initially speculated that a major source of discrepancy between time-domain signals recorded at different times would be due to changes in the ambient temperature. To

investigate this, an aluminium plate measuring 700mm x 500mm x 3mm thick was instrumented with a single pair of transducers of the type described previously and placed inside an environmental chamber.

The chamber was heated from ambient temperature of 22°C to 32°C and cooled back to ambient temperature three times over a total period of around 24 hours. This results in the temperature profile shown in Fig. 5(a). While the temperature cycling was taking place, time-domain signals were continuously recorded from the pair of transducers.

Using the very first signal as the baseline, the errors in the four zones described previously were recorded for all subsequent signals and the results are plotted in Fig. 5(b). It is immediately clear that the general error profile is intimately related to the temperature profile. It is also interesting to note that very early on in the experiment, the error level is significantly lower than that which is ever obtained at later times, even at nominally the same temperature. This is not a curiosity of the first cycle; a number of investigations have shown that this effect always occurs to signals recorded immediately after a baseline signal, regardless of which signal is chosen as the baseline.

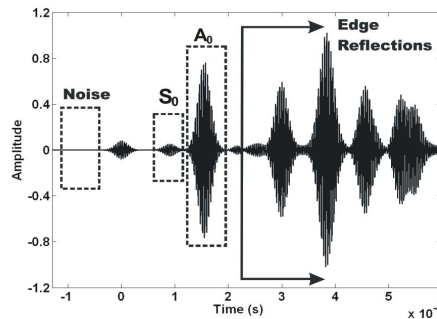


**Figure 4 :** Example time window illustrating the  $S_0$ ,  $A_0$  and Edge reflection zone

### 3.2 Discussion and modelling

The mechanisms that cause the change in error with temperature have been investigated and modelled. Temperature affects a number of important quantities: plate thickness, plate density, transducer separation, stiffness properties of plate and mechanical and electrical properties of transducer and bond layer.

Using Fourier synthesis it is readily possible to simulate the time-domain signals that are received for different material properties and propagation distances. From these error estimates can be calculated using the same procedure as used for experimental data. The largest effect is found to be caused by the change in elastic stiffness of the plate due to temperature which causes a change in ultrasonic velocity, which can be obtained from the literature [13].

Complete simulated signals can therefore be computed for the actual temperature profile seen experimentally, using the measured temperature to calculate the change in dimensions and elastic properties, and the measured centre frequency of the  $A_0$  signal to define the centre frequency of the simulated signal. The result is the direct comparison of measured error and simulated error shown in Figs. 6(a) and 6(b).

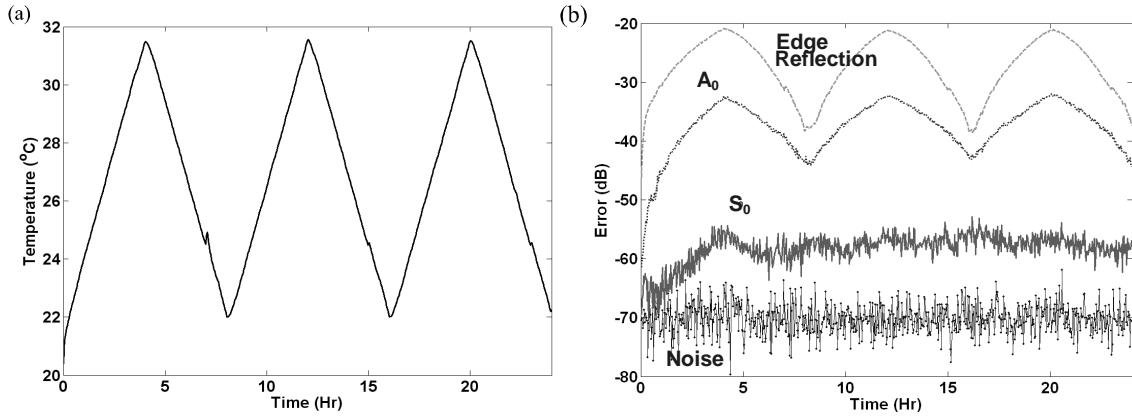


**Figure 5:** (a) Temperature variation during an experiment and (b) variation of error the course of the experiment in each of the zones shown in Figure 4.

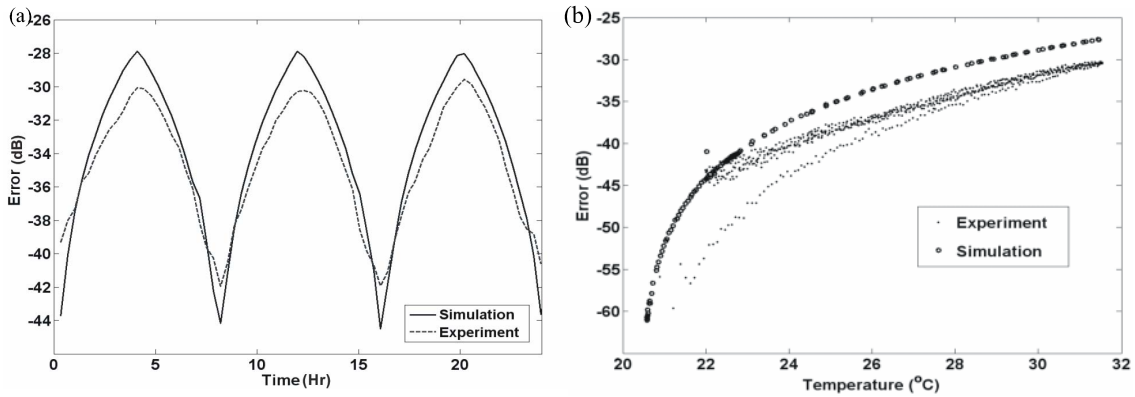


**Figure 6:** (a) Simulated and experimental error in the  $A_0$  zone due to change temperature (b) The simulated error vs. temperature plot overlaid on that of experimental results.

### 3.3 Techniques for improving the stability of the baseline subtraction approach

Other researchers have investigated methods for overcoming the effects of temperature. In particular, Lu and Michaels [14] describe an SHM methodology for use with diffuse waves in which, to overcome the effect of temperature the use of a database of baseline signals, as opposed to one baseline signal, is proposed. In this paper an approach similar to that of Lu and Michaels is implemented to reduce the effects of temperature on the long-term stability. This method is termed Optimal Baseline Subtraction (OBS) and the basic concept is as follows.

First a number of data-sets are recorded over a range of ambient conditions and these together form the baseline database. Subsequent signals are then compared to all signals in the baseline database until the best match is found and this signal is then subtracted. The OBS approach was applied to the data described in the previous section, using the time-domain signals captured over the first 8 hour temperature cycle as the baseline database. The resulting errors, using this database as the baseline for processing the remaining 16 hours of data, is shown in Fig. 7(a) using the same format as was used in Fig. 5(b). Comparison of these figures shows that the peak  $A_0$  error is reduced from around -35 dB to around -45 dB. A similar level of improvement of around 10 dB is seen in the other signals. It is important to note that OBS is not a “look-up table” approach based on

the measurement of ambient parameters and in fact will always give equal or superior performance to a look-up approach.

The same plate as used in Section 2.1 was placed in the environmental chamber and a similar cyclic heating regime was employed over 5 heating cycles. Prior to the fifth cycle, a 6.5mm diameter hole was drilled in the plate at a location away from the direct path between transducers. Data collected during the first two cycles was used as the baseline database for the OBS. The resulting error graphs for the remaining three temperature cycles are presented in Fig. 7(b).

As expected, the error is relatively low (below -40dB throughout for  $A_0$  direct transmission pulse and -30dB for the edge reflection) until the point when the damage is introduced. At this point there is a sudden rise to -20dB in the edge reflection zone error but no change in the  $A_0$  direct transmission error, since this is unaffected by the presence of the damage.

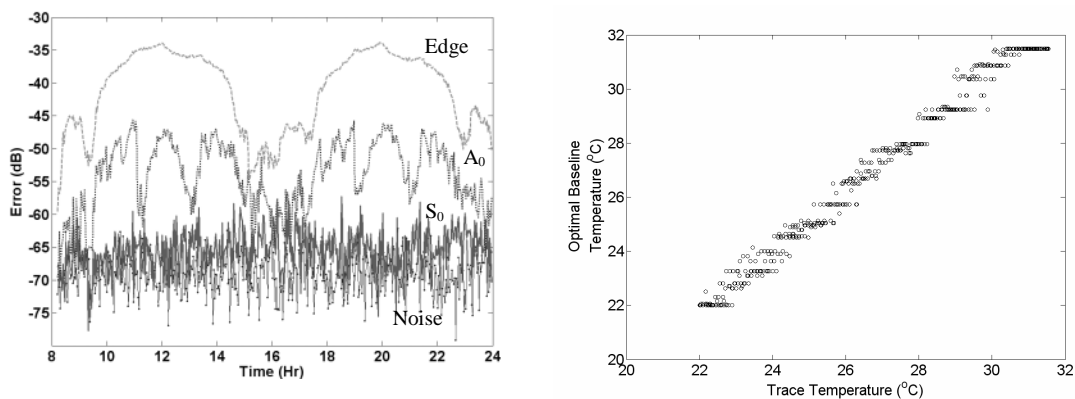


**Figure 7:** (a) Variation of error using OBS and (b) variation of error using OBS, showing an abrupt change in edge error at the point where damage was introduced into the structure indicated by the arrow.

## Conclusion

It has been noted that a viable SHM system requires a coherent noise floor in the final image at least 40 dB lower than the amplitude of the signal from an edge reflection. The crux of the baseline subtraction approach that determines the noise level in the final image is the stability of the subtraction itself. It has been shown that changes in signals associated with minor environmental fluctuations such as temperature changes of a few degrees are sufficient to produce coherent noise at around -25 dB, hence rendering the simple baseline subtraction technique unsuitable for practical SHM.

An improved approach, optimal baseline subtraction (OBS), where a database of baseline signals is used has been shown to be significantly better. In the context of the experiment described here where a single ambient parameter has been found to control stability the size of the baseline database is easily defined. In a real structure where multiple unknown parameters control stability it could be envisaged that the baseline database would be collected continuously until some predefined level of stability for matching new signals was reached.

## Acknowledgements

George Konstantinidis is funded by EPSRC through the Supergen 2 programme. The following companies provided additional financial support: Alstom Power,

Chromalloy UK Ltd, E.on, Howmet Ltd, Mitsui Babcock Energy Ltd, NPL, QinetiQ Ltd, Rolls Royce PLC, RWE nPower and Siemens Industrial Turbomachinery Ltd.

## References

- [1] Boller C 2001 Ways and options for aircraft structural health management *Smart Materials and Structures* **10**, 432-40
- [2] Le Clézio E, Castaings M and Hosten B 2002 The interaction of the S<sub>0</sub> Lamb mode with vertical cracks in an aluminium plate *Ultrasonics* **40** 192
- [3] Tua P S, Quek S T and Wang Q 2004 Detection of cracks in plates using piezo-actuated Lamb waves *Smart Materials and Structures* **13** 660
- [4] Jenot F, Ouaftouh M, Duquennoy M and Ourak M 2001 Corrosion thickness gauging in plates using Lamb wave group velocity measurements *Measurement Science and Technology* **12** 1293
- [5] Koh Y L, Chiu W K and Rajic N 2002 Effects of local stiffness changes and delamination on Lamb wave transmission using surface-mounted piezoelectric transducers *Composite Structures* **57** 443
- [6] Alleyne D, Pavlakovic B, Lowe M and Cawley P 2001 Rapid long-range inspection of chemical plant pipework using guided waves *Insight: Non-Destructive Testing and Condition Monitoring* **43** 93-6
- [7] Wilcox P P D 2003 Omni-directional guided wave transducer arrays for the rapid inspection of large areas of plate structures *IEEE transactions on ultrasonics, ferroelectrics, and frequency control* **50** 709
- [8] Wilcox P, Evans M, Pavlakovic B, Alleyne D, Vine K, Cawley P and Lowe M 2003 Guided wave testing of rail *Insight: Non-Destructive Testing and Condition Monitoring* **45** 420
- [9] Konstantinidis G, Wilcox P and Drinkwater B W 2005 Damage Detection Using a Distributed Array of Guided Wave Sensors (Orlando, Florida :SEM)
- [10] Konstantinidis G, Wilcox P D and Drinkwater B W 2005 The long term stability of guided wave structural health monitoring systems (Maine, Brunswick: American Institute of Physics)
- [11] Diligent O, Grahn T, Bostrom A, Cawley P and Lowe M J S 2002 The low-frequency reflection and scattering of the S<sub>0</sub> Lamb mode from a circular through-thickness hole in a plate: Finite element, analytical and experimental studies *Journal of the Acoustical Society of America* **112** 2601
- [12] Diligent O and Lowe M J S 2005 Reflection of the s<sub>0</sub> Lamb mode from a flat bottom circular hole *The Journal of the Acoustical Society of America* **118** 2879
- [13] Salama K and Ling C K 1980 Effect of stress on the temperature dependence of ultrasonic velocity *Journal of Applied Physics* **51** 1509
- [14] Lu Y and Michaels J E 2005 A methodology for structural health monitoring with diffuse ultrasonic waves in the presence of temperature variations *Ultrasonics* **43** 731